Chemical Engineering Science, Vol. 48, No. 13, pp. 2429–2441, 1993.
Printed in Great Britain.

0009–2509/93 $6.00 + 0.00

HYDROGENATION OF CYCLOHEXENE WITH $LaNi_{5-x}Al_xH_n$ METAL HYDRIDES SUSPENDED IN CYCLOHEXANE OR ETHANOL

E. D. SNIJDER, G. F. VERSTEEG† and W. P. M. VAN SWAAIJ
Twente University of Technology, Department of Chemical Engineering, PO Box 217, 7500 AE Enschede, The Netherlands

(*First received* 14 *August* 1992; *accepted in revised form* 8 *January* 1993)

Abstract—The hydrogenation of cyclohexene on the metal hydride forming alloys $LaNi_{4.8}Al_{0.2}$, $LaNi_{4.9}Al_{0.1}$ and $LaNi_5$, all suspended in cyclohexane and $LaNi_5$ suspended in ethanol, has been investigated. Two sources for hydrogen are recognized: hydrogen supplied by the gas phase and hydrogen which is available inside the metal hydride particles. For hydrogen which is supplied by the gas phase, the kinetics can be described with a two-site Langmuir–Hinshelwood relation, assuming a fast dissociative adsorption of hydrogen. The values of the rate constant, k_r, and adsorption coefficient for cyclohexene, $K_{C_6H_{10}}$, are lower if the hydrogenation is carried out on the metal (α) phase of the metal alloys instead of on the hydride (β) phase. Also, increasing the aluminum content results in a decrease of k_r and $K_{C_6H_{10}}$. In ethanol, a higher reaction rate constant and a lower adsorption coefficient were observed. The hydrogenation of cyclohexene with hydrogen provided by the metal hydride particles has been described with a combination of the rate equation for the hydrogenation and the relation for the hydrogen desorption from the hydride. It was found that the reaction rate decreases during the cyclohexene conversion, because the nature of hydride particles changes from the β into the α phase as the reaction proceeds. Initially, the hydrogenation is partly limited by the transport of hydrogen from the centre of the particle to the surface.

1. INTRODUCTION

Several metal alloys (e.g. FeTi, ZrNi, Mg_2Ni, $LaNi_5$) are able to form metal hydrides upon reaction with hydrogen. This reaction is reversible and proceeds mainly if the hydrogen pressure is above the equilibrium pressure P_{eq} of the metal alloy. The value of P_{eq} is characteristic for each alloy and depends on the composition of the alloy and on the temperature. Generally, the equilibrium pressure for hydrogen desorption from the metal hydride is lower than that for absorption in the metal. The amount of hydrogen absorbed by the metal is usually expressed with the storage capacity F, which is defined as the number of hydrogen atoms per atom of hydride-forming metal, e.g. La in $LaNi_5$. The maximum value of F for $LaNi_{5-x}Al_x$ alloys depends on the aluminum content and varies in a slurry roughly between 5.5 for $LaNi_5$ and 5.0 for $LaNi_{4.8}Al_{0.2}$.

Many applications based on the reversible hydrogen absorption capacity of these materials have been explored. Well-known examples exist in the use in hydrogen storage equipment (Reilly, 1977), hydrogen recovery units (Holstvoogd *et al.*, 1989) or in heat pumps (van Mal and Miedema, 1978). For more information on specific properties and applications of metal hydrides, the reader is referred to these articles.

Due to the active nickel component, application of these metal hydrides as catalysts also seems feasible. Soga *et al.* (1979) have reported on the hydrogenation of ethylene; more examples of gas-phase reactions are the synthesis of methanol (Baglin *et al.*, 1981), ammonia (Takeshita *et al.*, 1976) and the formation of hydrocarbons from CO and H_2 (e.g. Coon *et al.*, 1976; Shamsi and Wallace, 1983; Barrault *et al.*, 1986). Dehydrogenation reactions, where the metal alloys act as a hydrogen sink, have been reported, e.g. by Immamura *et al.* (1986, 1990) and Appelman *et al.* (1992).

Most of the work until now concerned gas-phase reactions, in some cases a mechanism for the hydrogenation with metal hydrides was proposed (e.g. Soga *et al.*, 1979). No such mechanistic study has been performed yet on hydrogenations with metal hydrides suspended in an organic solvent. Immamota *et al.* (1987) evaluated the applicability of $LaNi_5$ and $LaNi_{4.5}Al_{0.5}$ as catalysts for the hydrogenation of various organic compounds containing different functional groups. They carried out their experiments in a mixture of methanol and tetrahydrofuran (THF) and measured the conversion and selectivity after a certain reaction time. In the present study the kinetics and mechanism of cyclohexene hydrogenation with $LaNi_{5-x}Al_xH_n$ (with $x = 0, 0.1$ and 0.2) suspended in cyclohexane has been investigated. The effect of the solvent has been studied by comparing the results with experiments carried out with $LaNi_5$ in ethanol.

2. EXPERIMENTAL

2.1. *Theory*

The hydrogenation of cyclohexene in the presence of metal hydrides is schematically shown in Figure 1. Hydrogen is present both in the gas phase above the slurry and in the metal hydride particles. For the

†Author to whom correspondence should be addressed.

hydrogenation of adsorbed cyclohexene, two different sources for hydrogen can be recognized:

—hydrogen entering from the gas phase into the liquid, where it adsorbs on the catalyst: in this case the hydride acts merely as a conventional catalyst;
—hydrogen provided by the metal hydride: the hydride is now both catalyst and hydrogen source.

In the latter case, there is no need for additional hydrogen supply as long as the amount of hydrogen in the metal hydride is still sufficient. Figure 2 shows concentration profiles of dissolved hydrogen and cyclohexene in the slurry for the situation in which hydrogen is supplied by both the gas phase and the hydride. A part of the metal hydride has already been converted into the metal. The concentrations $C_{eq,a}$ and $C_{eq,d}$ denote hydrogen concentrations in the liquid corresponding to the equilibrium pressures of the metal hydride during absorption, $P_{eq,a}$, or desorption, $P_{eq,d}$. The hydrogenation process consists of several mass transfer and reaction steps:

(1) mass transfer of hydrogen from gas to liquid, $J_{H_2}a$;
(2) mass transfer of hydrogen from liquid bulk to the hydride particles (equal to $J_{H_2}a$ when $C_{H_2,l}$ is constant);
(3) adsorption of hydrogen on the surface of the hydride particles;
(4) dissociation of hydrogen molecules;
(5) mass transfer of cyclohexene from liquid bulk to the hydride particles;
(6) adsorption of cyclohexene on the surface of the hydride particles;
(7) transport of hydrogen atoms from the bulk to

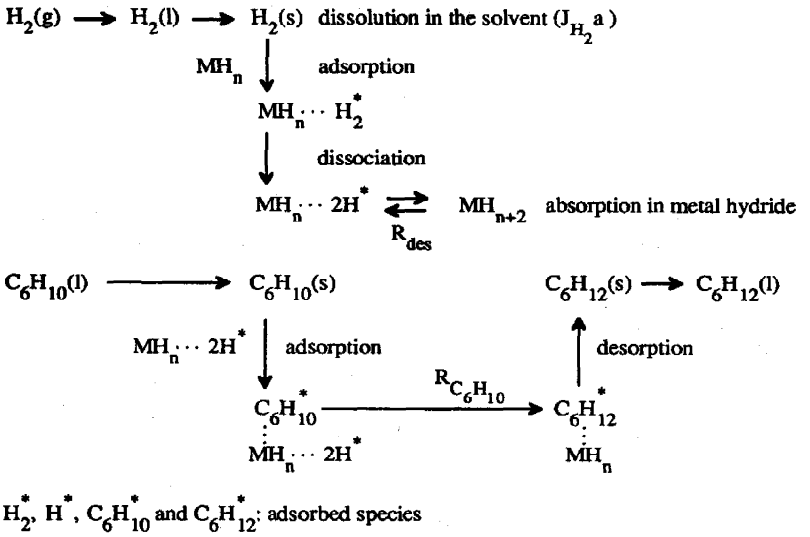

Fig. 1. Reaction scheme for cyclohexene hydrogenation.

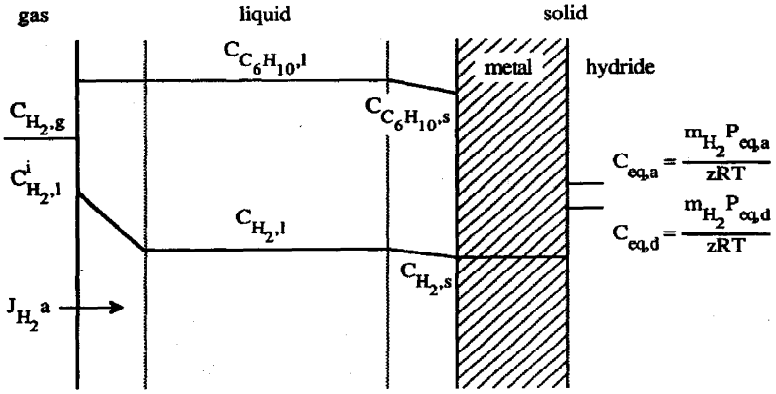

Fig. 2. Film model representation for cyclohexene hydrogenation in a slurry.

the surface of the metal hydride particles, R_{des};
(8) reaction between adsorbed hydrogen and cyclohexene, $R_{C_6H_{10}}$;
(9) desorption and mass transfer to the liquid of the formed cyclohexane.

Since hydrogen can be provided by the metal hydride or by the gas phase, the hydrogenation rate, $R_{C_6H_{10}}$, is equal to the sum of the hydrogen dissolution rate in the slurry, $J_{H_2}a$, and the rate of hydrogen desorption from the metal hydride, R_{des}:

$$R_{C_6H_{10}} = J_{H_2}a + R_{des}. \quad (1)$$

However, since all processes act simultaneously, it is rather difficult to distinguish between the rates of different steps. In order to determine the mechanism of cyclohexene hydrogenation on a metal hydride, all steps have to be measured separately. The mass transfer rates for hydrogen (steps 1 and 2) and a rate equation for the desorption applying to the same experimental conditions (e.g. pressure, temperature and stirrer speed) as used in the present study have been described elsewhere (Snijder *et al.*, 1992). The molar flows of the two components through the gas–liquid and liquid–solid interfaces follow the equations

$$J_{H_2}a = k_l a(C^i_{H_2,l} - C_{H_2,l}) \quad (2)$$

$$J_{H_2}a_s = k_s a_s(C_{H_2,l} - C_{H_2,s}) \quad (3)$$

$$J_{C_6H_{10}}a_s = k'_s a_s(C_{C_6H_{10},l} - C_{C_6H_{10},s}) = R_{C_6H_{10}}. \quad (4)$$

Desorption can be described with a shrinking-core relation (Snijder *et al.*, 1992)

$$1 - (1 - X)^{1/3} = k_d \ln\left(\frac{C_{eq,d}}{C_{H_2,s}}\right)t. \quad (5)$$

Here it has been assumed that the particles are spherical. The fraction reacted, X, is a function of the hydride capacity F according to

$$X = 1 - \frac{F}{F_0}. \quad (6)$$

The desorption rate R_{des} is related to dF/dt and, consequently, depends on k_d and $\ln(C_{eq,d}/C_{H_2,s})$. This will be discussed in more detail in Section 4.

In order to investigate the mechanism of the hydrogenation of cyclohexene, experiments were performed at two extreme conditions:

—hydrogen is supplied entirely by the gas phase: the metal hydride acts as a conventional catalyst;
—(almost) all hydrogen is supplied by the metal hydride; the metal hydride is both catalyst and hydrogen supplier.

The first set of experiments provides the actual information on the kinetics and the mechanism of the reaction on a hydride-forming metal alloy. Desorption of hydrogen from the metal hydride has to be prevented in this case as will be elucidated in Section 2.3. The second set of experiments was carried out in order to investigate the contribution of the hydrogen desorption rate from the metal hydride to the overall hydrogenation rate.

2.2. *Experimental set-ups and slurry preparation*

Two parallel, almost identical, experimental set-ups have been used for the experiments. Figure 3 gives a schematic flow-sheet of the most comprehensive version (set-up I). Snijder *et al.* (1992) have described the hydrogen handling and reactor part; the set-ups as

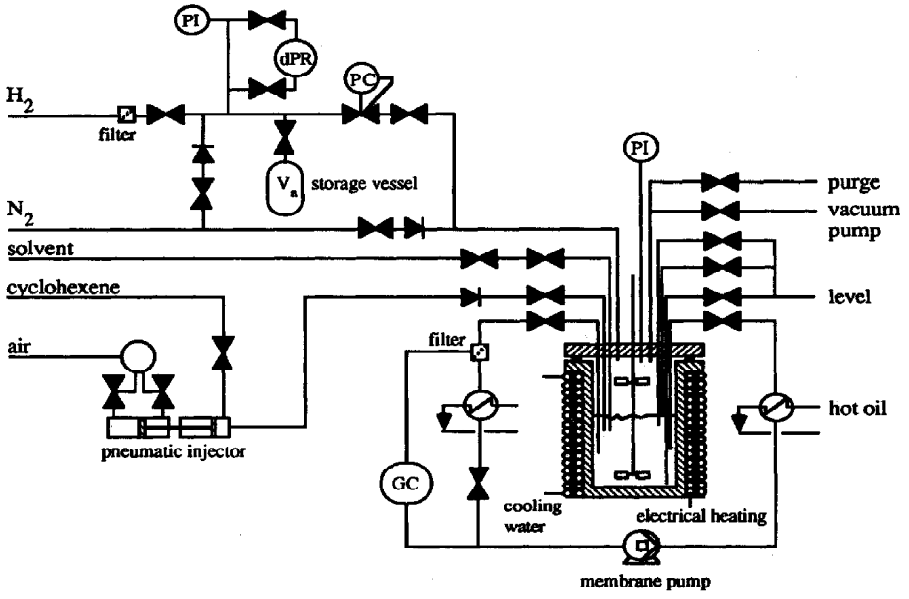

Fig. 3. Experimental set-up: PI = pressure indicator; GC = gas chromatograph; dPR = differential pressure recorder; PC = pressure controller.

used in the present study are extended with cyclohexene injection and sampling equipment. The pretreatment of cyclohexene is similar to that of the other solvents (storage on mol sieves, degassing with oxygen-free nitrogen), but it is first passed through a column filled with active carbon and then, after the degassing, distilled in a 2 m long packed column under nitrogen atmosphere to remove small traces of stabilizer added by the supplier.

Cyclohexene injection is carried out with a pneumatic injector (set-up I) or with the help of a measuring tube (set-up II). The major difference between the two set-ups is the way of sampling. Set-up I contains a sample loop: the slurry is circulated with a membrane pump (Lewa EKM1-V) along a filter back into the reactor. A small stream of clean liquid flows through the filter, passes the sampling valve (1 μl internal sample loop) of a gas chromatograph (Varian 3400) and then flows back again into the main stream. Automatic sampling is performed by switching the valve. The time for a sample to flow from the reactor to the sampling valve was determined with residence time distribution experiments and was of negligible duration (about 3 s) in comparison with the reaction times (several hundred seconds). Samples from the reactor of the second set-up are taken through a capillary tube with a small filter at the end. The samples were injected by hand into the gas chromatograph.

The properties of the slurries, the suppliers of the chemicals and metal alloys and the activation method of the metal alloys have been given in detail by Snijder *et al.* (1992). Some characteristic properties of the metal hydrides (molar mass, surface area, density and average particle diameter, again based on spherical particles) are given in Table 1; Table 2 lists the experimental conditions applied.

2.3. *Experimental procedure*

First the experimental procedure is described for the determination of the hydrogenation kinetics of the reaction with hydrogen provided by the gas phase. The nature of the metal depends on the hydrogen pressure applied. At pressures above the absorption equilibrium pressure, $P_{eq,a}$, the metal alloy is saturated with hydrogen and the solid material is in the hydride (β) phase. Hydrogen desorption will occur if the concentration close to the metal surface, $C_{H_2,s}$, falls below the desorption equilibrium concentration, $C_{eq,d}$. Consequently, experiments above the equilibrium pressure have to be carried out at a high stirring speed (high mass transfer rates) and constant hydrogen pressure in order to keep the liquid saturated at concentrations above $C_{eq,d}$. If the applied hydrogen pressure is below the desorption equilibrium pressure, $P_{eq,d}$, the metal alloy contains only a small amount of absorbed hydrogen and it is in the metal (α) phase. No hydrogen desorption from the hydride can take place at such hydrogen pressures.

The hydrogenation is carried out as a batch experiment. After injection of a well-defined volume of cyclohexene, the pressure in the reactor is kept constant within about 0.02 bar by adding the consumed amount of hydrogen from a storage vessel, V_a, via a pressure reduce valve. The reactor temperature and the pressure in the storage vessel are recorded and samples are taken from the slurry. The hydrogen consumption rate can be calculated according to

$$J_{H_2}a = -\frac{V_a}{z_a R T_a V_{sl}} \frac{dP_a}{dt}. \quad (7)$$

Since, for quasi steady-state conditions, both molar flows as given by eqs (2) and (3) are equal to $J_{H_2}a$ ($C_{H_2,l}$ is then constant), $C_{H_2,l}$ can be eliminated. Assuming that the gas and liquid phases are in equilibrium at the interface, $C^i_{H_2,l}$ can be obtained with Henry's law. The gas-phase hydrogen concentration $C_{H_2,g}$ is calculated according to the gas law; the vapour pressure of cyclohexane has been taken into account:

$$C^i_{H_2,l} = m_{H_2} C_{H_2,g} \quad \text{with } C_{H_2,g} = \frac{P_r - P_{vap}}{z_r R T_r}. \quad (8)$$

Table 1. Some properties of the metal alloys

Material	M_{hydr} (kg/mol)	A_{hydr} (m^2/kg)	ρ_{hydr} (kg/m^3)	$d_p \times 10^6$ (m)
$LaNi_{4.8}Al_{0.2}$	0.4261	360	8110	6
$LaNi_{4.9}Al_{0.1}$	0.4293	300	8200	9
$LaNi_5$	0.4325	310	8290	11

Table 2. Experimental conditions

	Volume (m^3)			Conditions
	set-up I	set-up II	T_r	293–333 K
V_l	620.6×10^{-6}	312.2×10^{-6}	P_r	3–25 bar
V_g	317.4×10^{-6}	238.6×10^{-6}	n	set-up I: high: 2000 rpm
V_a	1607.5×10^{-6}	1106.4×10^{-6}		low: 900 rpm
				set-up II: 1000 rpm

Substitution of $C^i_{H_2,l}$ according to eq. (8) into eq. (2) then gives an expression for $C_{H_2,s}$:

$$C_{H_2,s} = \frac{m_{H_2} P_{H_2}}{z_r R T_r} - J_{H_2} a \left(\frac{1}{k_l a} + \frac{1}{k_s a_s} \right). \quad (9)$$

The experimental procedure for the determination of the mass transfer coefficients, $k_l a$ and $k_s a_s$, and the results of these experiments have been presented by Snijder *et al.* (1992). Liquid samples which were taken during a hydrogenation experiment provide the cyclohexene concentrations. The hydrogenation rate can be derived from

$$R_{C_6H_{10}} = -\frac{dC_{C_6H_{10}}}{dt}. \quad (10)$$

In the situation in which hydrogen is provided by the hydride, the metal particles are first completely saturated with hydrogen. Experiments were carried out at lower stirrer speeds. Shortly before the cyclohexene injection, the hydrogen pressure was reduced to the absorption equilibrium pressure of the metal hydride at reaction temperature. No additional hydrogen was supplied to the reactor. In this situation the hydrogen flow into the liquid is very small, due to the small driving force for absorption and the low mass transfer coefficient. The reactor pressure and temperature were recorded; during the reaction, liquid samples were taken.

3. RESULTS

3.1. *Introduction*

Cyclohexene hydrogenation was investigated with several metal hydrides and solvents. The first experiments concern the reaction with $LaNi_5H_n$ ($n = 4.5$–5.5 for values of $P_{H_2} > P_{eq,a}$ and $n \approx 0$ when $P_{H_2} < P_{eq,d}$) in order to obtain the mechanism and kinetics of the reaction. Next, cyclohexene has been hydrogenated with hydrogen provided by the $LaNi_5$ hydride. Furthermore, the effect of nickel substitution by aluminum has been studied. Experiments were carried out with $LaNi_{4.8}Al_{0.2}$ and $LaNi_{4.9}Al_{0.1}$. These alloys have lower equilibrium pressures than the original $LaNi_5$. Finally, cyclohexene was hydrogenated with $LaNi_5$ suspended in ethanol in order to investigate the effect of the solvent.

3.2. *Hydrogenation of cyclohexene with* $LaNi_5H_n$ *suspended in cyclohexane*

3.2.1. *Hydrogen provided by the gas phase.* As elucidated in Section 2.3, these experiments were carried out at high stirrer speeds and a constant hydrogen pressure. The cyclohexene concentration during the reaction can be calculated from the injected amount of cyclohexene and corrected for the amount of hydrogen consumed. Figure 4 gives an example at 313 K and 16 bar. A comparison between the calculated concentrations and the concentration of cyclohexene in the samples that were taken (included in Fig. 4 as well) shows that the concentrations in the samples are just somewhat below the calculated values. The slopes

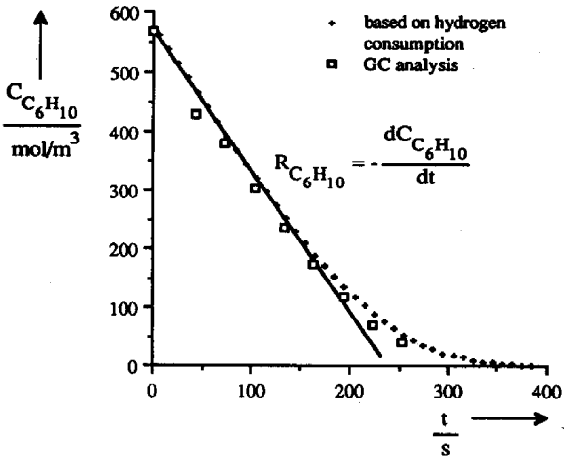

Fig. 4. Concentration of cyclohexene vs time when hydrogen is provided by the gas phase, $T_r = 313$ K, $P_r = 16$ bar, $n = 2000$ rpm.

of both the curves are identical; consequently, it can be concluded that after a short induction period, hydrogen is provided by the gas phase. Initially, a small amount of cyclohexene was apparently converted, with hydrogen provided by the metal hydride. The hydrogenation rate of cyclohexene (slope of the curve) is constant at high cyclohexene concentrations and decreases at an increasing conversion. Similar behaviour was observed for other temperatures and pressures; the reaction order for cyclohexene obviously increases from zero initially to higher values at decreasing cyclohexene concentrations.

In order to obtain the reaction order in hydrogen, the hydrogen pressure was varied between 3 and 25 bar at various temperatures. The reaction rate of cyclohexene, $R_{C_6H_{10}}$, is for these experimental conditions equal to the hydrogen consumption rate, $J_{H_2}a$. In the region with a zero reaction order in cyclohexene $J_{H_2}a$ can be calculated with eq. (7), as demonstrated with the initial slope of the line in Fig. 4. The hydrogen concentration close to the surface, $C_{H_2,s}$, was determined by using eq. (9); Fig. 5 shows the results at 333 K. Between 32 and 39 mol/m^3 there is a sharp discontinuity in the curve; these concentrations correspond to the equilibrium concentration for desorption and absorption, respectively, at 333 K ($P_{eq,d} = 6.6$ bar, $P_{eq,a} = 8.1$ bar), which are included in Fig. 5 as well. Due to the high mass transfer coefficient $k_s a_s$, the value of $C_{H_2,s}$ appeared to be almost identical to the hydrogen concentration in the bulk of the liquid. However, for convenience, it was then assumed that the cyclohexene concentration close to the metal surface could also be considered equal to the bulk concentration $C_{C_6H_{10}}$.

An explanation for the discontinuity in the reaction rate is the change in the nature of the alloy, which is dependent on the hydrogen pressure applied. As long as $C_{H_2,s} > C_{eq,a}$ (high-pressure experiments), the alloy remains in the β phase and cyclohexene is hydrogenated on the hydride surface, whereas at surface

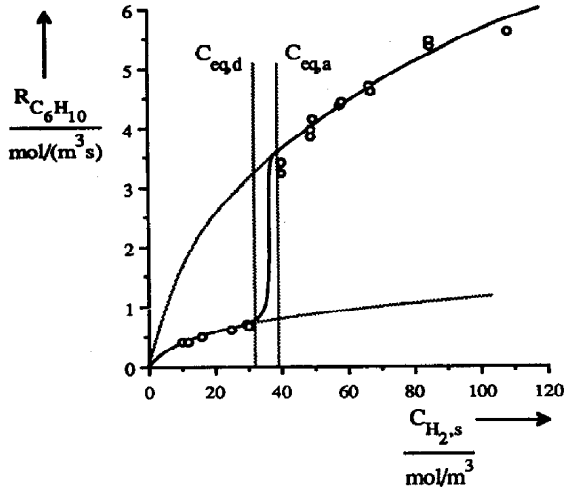

Fig. 5. Reaction rate vs the hydrogen concentration close to the surface, $T_r = 333$ K, $n = 2000$ rpm.

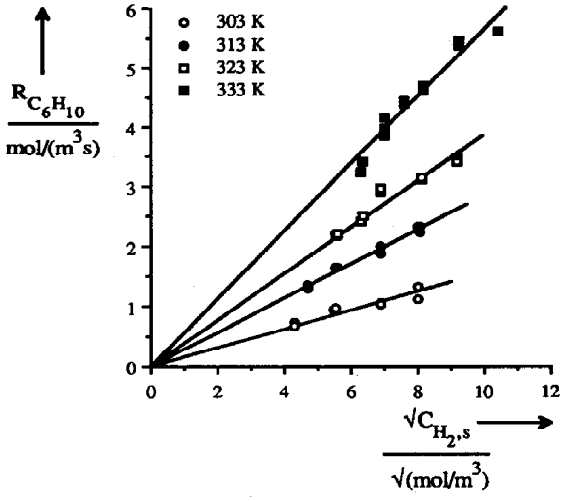

Fig. 6. Reaction rate on $LaNi_5$ vs $\sqrt{C_{H_2,s}}$, at hydrogen pressures above the equilibrium pressure.

concentrations below $C_{eq,d}$ (low-pressure experiments) cyclohexene is hydrogenated on the metal. It also appeared that, although the reaction order for cyclohexene is initially zero both on the hydride and on the metal surface, the change in reaction order takes place at a lower cyclohexene conversion on the metal than on the hydride.

The reaction order for hydrogen can be obtained by plotting ln ($R_{C_6H_{10}}$) against ln ($C_{H_2,s}$). The slope of the curve is approximately 1/2, indicating a reaction order in hydrogen of one-half. Figure 6 shows the half order dependence for temperatures between 303 and 333 K. Since the equilibrium pressures of $LaNi_5$ become too low at low temperatures, the hydrogenation on the metal phase could be investigated at several pressures only at 333 K. The reaction order appeared to be one-half as well. The slopes of the lines in Fig. 6 yield the reaction rate constants for the metal hydride. For the metal the rate constants have been obtained by dividing the rate $R_{C_6H_{10}}$ by $\sqrt{C_{H_2,s}}$. The rate constants k_r are formally taken per unit of external surface area and then multiplied by the specific liquid–solid interfacial area a_s in order to obtain a reaction rate per volume slurry. The equation which describes the hydrogenation at high cyclohexene concentrations reads

$$R_{C_6H_{10}} = k_r a_s \sqrt{C_{H_2,s}}. \qquad (11)$$

Figure 7 shows the temperature dependence of the rate constants divided by ε_s, giving the following Arrhenius relations:

Reaction on metal surface:

$$\frac{k_r a_s}{\varepsilon_s} = 3.69 \times 10^6 \exp\left(\frac{-34.9 \times 10^3}{RT}\right)$$

Reaction on hydride surface:

$$\frac{k_r a_s}{\varepsilon_s} = 21.1 \times 10^6 \exp\left(\frac{-35.5 \times 10^3}{RT}\right).$$

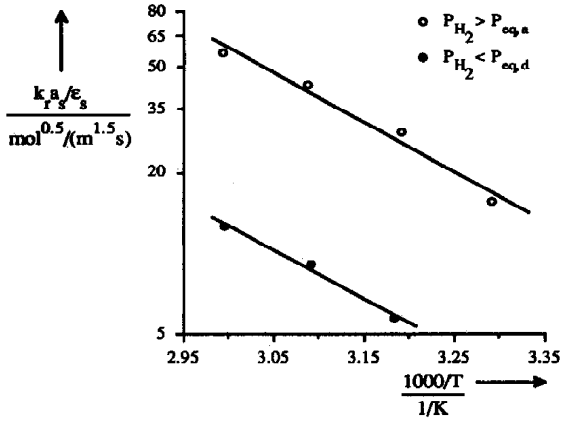

Fig. 7. Temperature dependence of the reaction rate constants for the hydrogenation of cyclohexene on $LaNi_5H_n$.

It seems that the activation energies for the hydrogenation of cyclohexene on the hydride and on the metal phase of $LaNi_5$ are equal within the range of experimental accuracy.

3.2.2. *Hydrogen provided by the metal hydride.* At 333 K cyclohexene was hydrogenated with hydrogen which was provided by the metal hydride, the reactor pressure was initially 8.1 bar. The cyclohexene concentration as a function of the reaction time for such an experiment is illustrated in Fig. 8(a). During the reaction, the reactor pressure decreased as shown in Fig. 8(b). The corresponding amount of hydrogen which is provided by the gas phase is about 6% of the total amount required for the cyclohexene conversion. This means that almost all hydrogen is provided by the $LaNi_5H_n$. The change in the hydrogen absorption

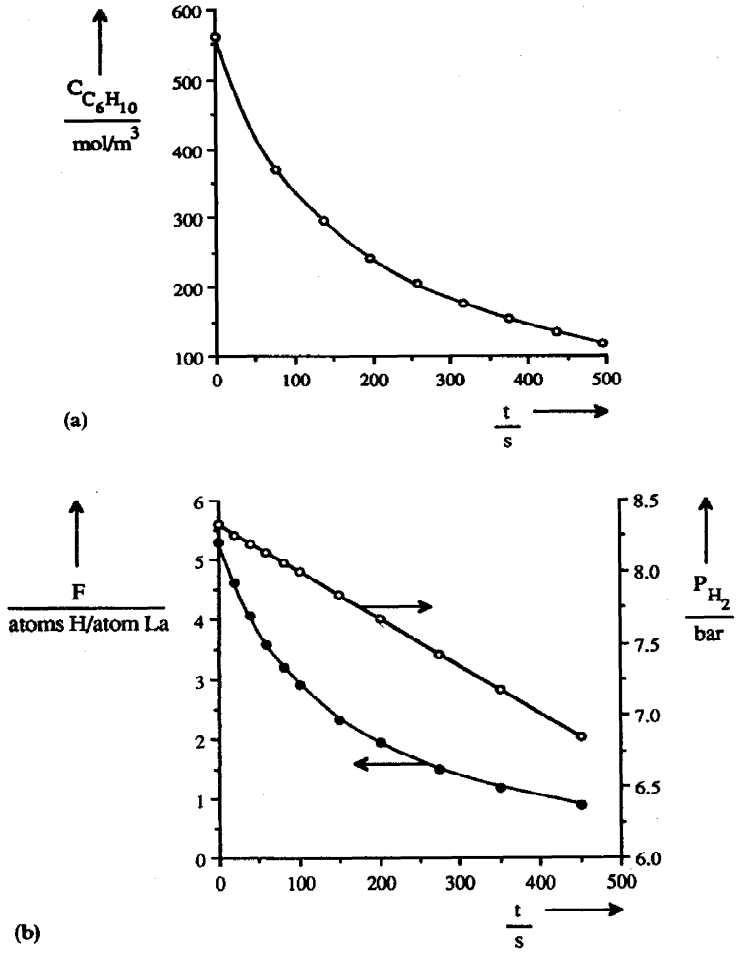

Fig. 8. (a) Concentration of cyclohexene vs time when hydrogen is provided by the metal hydride, $T_r = 333$ K, $n = 900$ rpm. (b) Hydrogen storage capacity F and the reactor pressure vs time.

capacity F of the metal hydride can be derived from

$$F(t) = F_0 - \frac{2}{n_{hydr}}\left[(C_{C_6H_{10},0} - C_{C_6H_{10}}(t))(1-\varepsilon_s)V_{sl} - \frac{[P_{r,0} - P_r(t)]V_{r,g}}{z_r R T_r}\right]. \quad (12)$$

The result of these calculations is also depicted in Fig. 8(b). In contrast to the experiments where hydrogen is provided by the gas phase (Fig. 4), there appears to be no region where the reaction rate is constant; in fact, it decreases continuously as the reaction proceeds. This will be discussed in more detail in section 4.

3.3. *Influence of aluminum in* $LaNi_{5-x}Al_x$

The nickel in $LaNi_5$ can be substituted by aluminum up to a maximum of $LaNi_{3.5}Al_{1.5}$. This leads to a decrease of both the equilibrium pressures and the maximum absorption capacity. However, the stability of the material against disproportionation and subsequent loss of absorption capacity reduces if aluminum is present in the alloy (Goodell, 1984). Hydrogenation experiments with $LaNi_{4.8}Al_{0.2}$ and $LaNi_{4.9}Al_{0.1}$ at hydrogen pressures above the absorption equilibrium pressure have produced comparable results as obtained with $LaNi_5$. The reaction order in cyclohexene was again initially zero and increases at decreasing cyclohexene concentration; however, the change in reaction order occurs at lower cyclohexene conversions. For hydrogen the reaction order was again one-half. There appeared to be a considerable difference in activities among the three alloys; Fig. 9 gives the results. The following Arrhenius relations have been derived for the reaction rate constants:

Reaction on $LaNi_{4.8}Al_{0.2}$:

$$\frac{k_r a_s}{\varepsilon_s} = 18.4 \times 10^6 \exp\left(\frac{-39.0 \times 10^3}{RT}\right)$$

Reaction on $LaNi_{4.9}Al_{0.1}$:

$$\frac{k_r a_s}{\varepsilon_s} = 3.69 \times 10^6 \exp\left(\frac{-31.9 \times 10^3}{RT}\right).$$

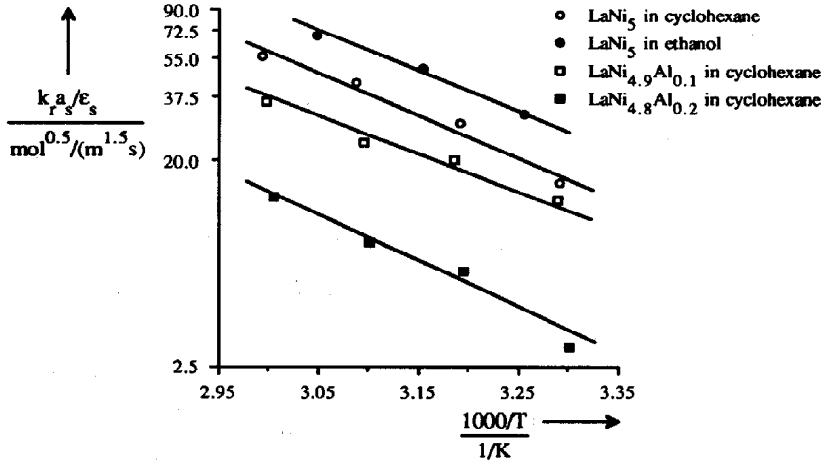

Fig. 9 Influence of the aluminum content in $LaNi_{5-x}Al_x$ and the solvent on the activity of the metal hydrides for cyclohexene hydrogenation.

The differences between the activation energies for the hydrogenation of cyclohexene on the β phase of the alloys are only small: 39.0, 31.9 and 35.5 kJ/mol for $LaNi_{4.8}Al_{0.2}$, $LaNi_{4.9}Al_{0.1}$ and $LaNi_5$, respectively.

Since the equilibrium pressures of the aluminum-containing alloys are much lower, it was only possible to carry out the experiments at pressures below $P_{eq,d}$ at 323 and 333 K and 3 bar. The results indicated again that the activity is strongly reduced when cyclohexene is hydrogenated on the metal phase of the alloys instead of on the hydride phase; however, there are too few datapoints to derive Arrhenius relations for the rate constants.

3.4. *Influence of the solvent*

With $LaNi_5$ several experiments were carried out in ethanol as solvent. After every reaction, the solvent and the reaction product were flushed out of the reactor and the reactor was refilled with ethanol; the metal alloy remained in the reactor. The reaction orders in hydrogen and cyclohexene are identical to those in cyclohexane as solvent. A comparison between the activity of $LaNi_5$ in cyclohexane and ethanol is included in Fig. 9, the activity in ethanol appeared to be higher than in cyclohexane. The rate constant was found to obey

Reaction on $LaNi_5$ in ethanol:

$$\frac{k_r a_s}{\varepsilon_s} = 15.1 \times 10^6 \exp\left(\frac{-33.4 \times 10^3}{RT}\right)$$

Snijder *et al.* (1992) have reported that for hydrogen absorption in $LaNi_5$ suspended in the same solvents, the highest reaction rate constant was also obtained in ethanol. The influence of the solvent is obviously the same for both hydrogen absorption and cyclohexene hydrogenation. The activation energy is once again almost identical to the values obtained for the hydrogenation in the other slurries.

4. DISCUSSION

The results showed that the reaction order for cyclohexene increases from zero to higher values at decreasing cyclohexene concentration; this was also influenced by the aluminum content and the state of the alloy (α or β phase). The reaction order for hydrogen is one-half in the zero-order region of cyclohexene for all metal alloys and both solvents at every applied temperature.

A mechanism which can describe these phenomena is based on the reaction scheme for the hydrogenation of an olefin, which was originally proposed by Polanyi and Horiuti. They assumed that the hydrogenation of a certain olefin (A) consists of four steps, where * denotes a free-surface site:

Step 1: $A + 2^* \rightleftharpoons {}^*A^*$

Step 2: $H_2 + 2^* \rightleftharpoons 2H^*$

Step 3: ${}^*A^* + H^* \rightleftharpoons AH^* + 2^*$

Step 4: $AH^* + H^* \xrightarrow{k_4} AH_2 + 2^*.$

Boudart and co-workers presented a series of studies on the hydrogenation of cyclohexene, both for gas- and liquid-phase reactions, on supported Pd and Pt catalysts (Segal *et al.*, 1978; Madon *et al.*, 1978; Gonzo and Boudart, 1978). They evaluated several rate equations with a different rate-limiting step in this mechanism and concluded that at high pressure and temperature step 4 is rate-limiting and the first three steps are in equilibrium, resulting in a reaction order for hydrogen of one-half. Surface coverages of cyclohexene and hydrogen in the present study have been estimated by assuming Langmuir-type adsorption isotherms. If hydrogen adsorbs dissociatively on metal hydrides as well, two general rate equations can be derived, depending upon whether hydrogen and cyclohexene are thought to adsorb on the same type of active site or on two different sites:

One-site model:

$$R_{C_6H_{10}} = k_4 a_s \frac{K_{H_2}\sqrt{C_{H_2,s}}K_{C_6H_{10}}C_{C_6H_{10}}}{(1 + K_{H_2}\sqrt{C_{H_2,s}} + K_{C_6H_{10}}C_{C_6H_{10}})^2} \quad (13)$$

Two-site model:

$$R_{C_6H_{10}} = k_4 a_s \frac{K_{H_2}\sqrt{C_{H_2,s}}}{(1 + K_{H_2}\sqrt{C_{H_2,s}})} \frac{K_{C_6H_{10}}C_{C_6H_{10}}}{(1 + K_{C_6H_{10}}C_{C_6H_{10}})}. \quad (14)$$

Based on the experimentally found change in reaction order for cyclohexene, it can be concluded that two different active sites are present on the surface, since a single-site model [eq. (13)] would predict a negative reaction order at high cyclohexene concentrations. Soga *et al.* (1979) have examined the hydrogenation of ethylene on $LaNi_5$ and also concluded that two different sites had to be present. The existence of two surfaces regions has been proposed, among others, by Wallace *et al.* (1979), who have found that on the surface of $LaNi_5$, after oxidation followed by reduction with hydrogen, La_2O_3 [or $La(OH)_3$] and Ni precipitates are formed. Hydrogen is thought to adsorb on the nickel sites, whereas cyclohexene may adsorb on the La_2O_3 sites.

The experimentally observed reaction orders can be obtained assuming that $K_{H_2}\sqrt{C_{H_2,s}} \ll 1$ (weakly bonded hydrogen). Consequently, the equation which describes the hydrogenation of cyclohexene on $LaNi_{5-x}Al_xH_n$ metal hydrides in either cyclohexene or ethanol reads

$$R_{C_6H_{10}} = k_4 a_s K_{H_2}\sqrt{C_{H_2,s}} \frac{K_{C_6H_{10}}C_{C_6H_{10}}}{1 + K_{C_6H_{10}}C_{C_6H_{10}}}. \quad (15)$$

At high cyclohexene concentrations, zero reaction order in cyclohexene can be observed and the apparent rate constant k_r in eq. (11) appears to be equal to $k_4 K_{H_2}$. Competitive adsorption of the solvents on either of the two or on both types of surfaces will lead to a reduction of the reaction rate. Since the lowest rates were measured in cyclohexane, it is to be expected that cyclohexane is bonded more strongly on the surface. Some authors (e.g. Martin and Imelik, 1974; Chesters *et al.*, 1986) suggest that, due to C–H · · · M interactions, the bond between hydrocarbons and a metal surface (Ni, Cu, Pd) is indeed relatively strong.

With the experimentally determined dependency of the reaction rate ($R_{C_6H_{10},exp}$) and cyclohexene concentration, the adsorption coefficient for cyclohexene $K_{C_6H_{10}}$ and the reaction rate constant $k_r a_s$ can be fitted by minimization of $\chi^2 = (R_{C_6H_{10},exp} - R_{fit})^2$. R_{fit} is calculated according to eq. (15). As elucidated previously, the reaction rate $R_{C_6H_{10}}$ is equal to the hydrogen consumption rate $J_{H_2}a$, which can be determined with eq. (7). At the highest cyclohexene concentrations, the reaction rates as determined according to Fig. 4 have been used. For this two-parameter, one-dimensional fit problem, the method of Nealder Mead was applied (Press *et al.*, 1986). The competitive adsorption of solvent molecules on the surface was not taken into account in these calculations.

A comparison between the experimentally determined dependence of $R_{C_6H_{10}}$ and $C_{C_6H_{10}}$ and the rates which have been calculated according to eq. (15) and the fitted $k_r a_s$ and $K_{C_6H_{10}}$ is shown in Fig. 10. The correspondence, especially at low concentrations, is very good. The deviation between the fitted and the experimentally determined curves at the highest concentrations is due to the fact that the reaction rates were approximated with a zero reaction order dependency on cyclohexene, which appears to be, according to Fig. 10, not completely correct. Using this method, the adsorption coefficient for cyclohexene can be determined for all the temperatures studied. The adsorption coefficients on $LaNi_{4.9}Al_{0.1}$ and $LaNi_5$ suspended in cyclohexane or ethanol were fitted at a pressure of 12 bar. Since for $LaNi_{4.8}Al_{0.2}$ most of the experiments were carried out at 8 bar, these data have been used. The results are presented in Fig. 11(a). Figure 11(b) shows the influence of the aluminum content and solvent. Average values for the fitted $k_r a_s$ and $K_{C_6H_{10}}$ are listed in Table 3. The adsorption coefficient for cyclohexene is influenced by the nature of the surface and the type of solvent. A higher aluminum content in the metal alloys leads to a decrease of the adsorption coefficient. Moreover, a reduction of the adsorption coefficient on $LaNi_5$ has been observed if this material changes into the α phase. Finally, ethanol instead of cyclohexane as solvent resulted in a lower adsorption coefficient.

The slope of the curves in Fig. 11 is according to e.g. Bond (1962) equal to $-\Delta H_a/R$, with ΔH_a the heat of adsorption. The calculated values for the $-\Delta H_a$ (5–6 kJ/mol) were almost identical for all hydrides. The magnitude of $-\Delta H_a$ is low in comparison with values obtained for adsorption of several comparable components out of the gas phase on a nickel surface.

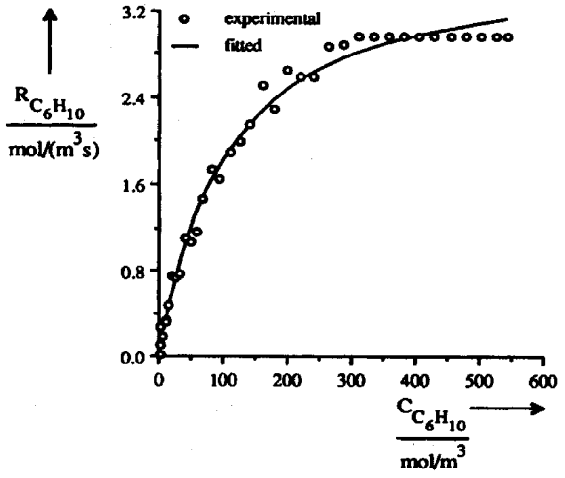

Fig. 10. Experimental and fitted reaction rates of cyclohexene hydrogenation on $LaNi_5$ at 323 K and 12 bar.

Table 3. Fitted data for cyclohexene hydrogenation on several metal hydrides: $k_r a_s$ and $K_{C_6H_{10}}$

System	T_r (K)	$k_r a_s/\varepsilon_s$ [mol$^{0.5}$/(m$^{1.5}$ s)]	$1000 \times K_{C_6H_{10}}$ (m^3/mol)
$LaNi_5$ (α phase)	314.0	8.2	5.4
	324.0	12.6	5.7
	333.0	17.8	5.2
$LaNi_5$ (β phase)	303.8	18.8	10.8
	313.2	35.8	9.3
	322.8	53.3	9.6
	335.0	74.9	9.1
$LaNi_5$ (in ethanol)	307.0	55.9	1.8
	317.0	83.6	2.4
	327.3	120.8	1.6
$LaNi_{4.9}Al_{0.1}$	303.8	18.8	5.6
	313.8	27.9	5.6
	323.0	34.7	4.9
	333.0	52.7	4.7
$LaNi_{4.8}Al_{0.2}$	312.1	10.5	3.2
	322.7	16.1	3.8
	332.9	26.2	2.7

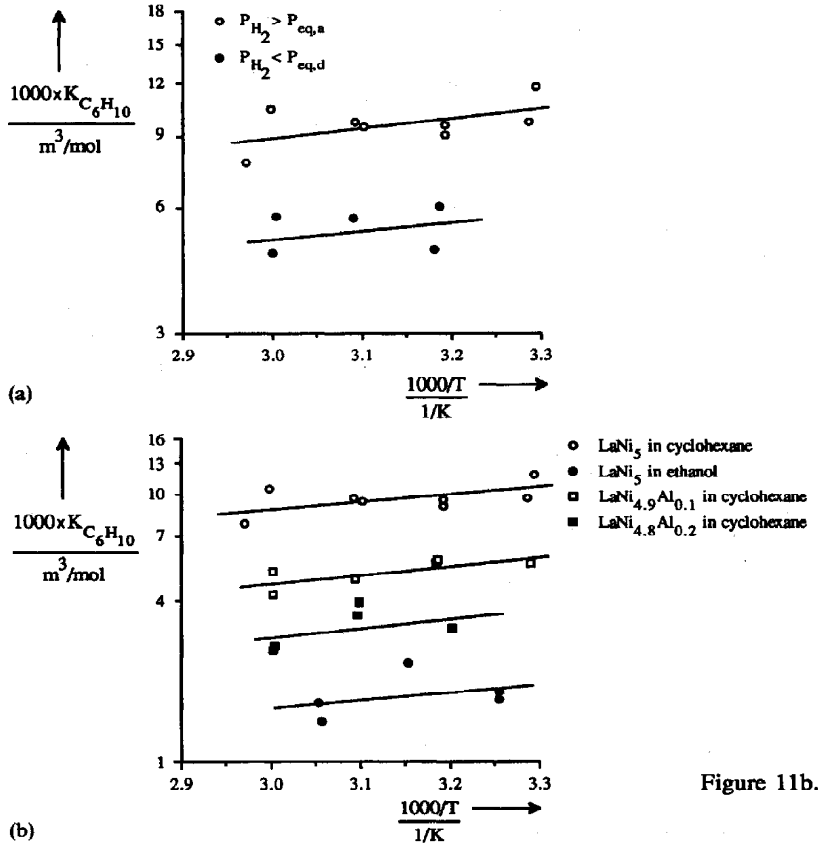

Figure 11b.

Fig. 11. Adsorption coefficients of cyclohexene on $LaNi_{4.8}Al_{0.2}$, $LaNi_{4.9}Al_{0.1}$ and $LaNi_5$.

Svoboda *et al.* (1970) reported values for $-\Delta H_a$ between 43 and 64 kJ/mol for adsorption of benzene on several types of Raney nickel. Barbernics and Tétényi (1972) have carried out investigations on benzene and cyclohexane adsorption on nickel and nickel oxide surfaces and concluded that the ΔH_a was almost equal for both compounds. Their values for $-\Delta H_a$ vary between 18 and 28 kJ/mol, depending upon temperature and coverage. The difference between the $-\Delta H_a$ values as obtained in the present study and in the

other investigations may be attributed to the fact that in the present study the cyclohexene is in the liquid phase and surrounded by solvent molecules. The difference between the two ΔH_a values should then be about equal to the heat of solvation of gaseous cyclohexene into cyclohexane or ethanol. This heat of solvation is related to the heat of condensation of cyclohexene (≈ -33 kJ/mol); the agreement is apparently fairly good.

From the results it can be concluded that the hydrogenation includes adsorption of hydrogen and cyclohexene on two different surface sites, which are assumed to be Ni and La_2O_3 [or $La(OH)_3$] regions. This implies that the reaction can take place only on the boundary between these regions. As elucidated above, the rate-limiting step in the reaction is the addition of the second hydrogen atom to the half-hydrogenated cyclohexene molecule. Since it was observed that the activation energy was almost independent of the aluminum content in the hydride, type of solvent or state of the alloy (α or β phase), it can be concluded that the nature of the surface regions where the reaction takes place is unaffected by these parameters. The lower reaction rates on the aluminum-containing alloys can then be explained by assuming that Al_2O_3 is present on the boundary between the reactive La_2O_3 and Ni sites. The reaction area is consequently smaller and the hydrogenation rate decreases. When the alloy is in the β phase, more nickel sites might be in an activated state, resulting in a higher reaction rate. Finally, the presence of these Al_2O_3 regions results in a lower adsorption coefficient for cyclohexene on the surface. The lower adsorption coefficient of cyclohexene in ethanol as solvent indicates that the binding strength between cyclohexene and $LaNi_5$ is weaker in ethanol than in cyclohexane. This may be the reason for the higher reaction rate in ethanol.

The hydrogenation of cyclohexene with hydrogen provided by the $LaNi_5$ proceeds according to a different mechanism. The reaction rate of cyclohexene, which, according to eq. (10), is equal to the slope of the curve in Fig. 8(a), decreases continuously. In order to describe this process, the rate equation for the hydrogenation as derived above and the relation for the desorption of hydrogen form the hydride particles have been combined. Equations (5) and (6) give the relation between F and $C_{H_2,s}$, $C_{eq,d}$, k_d and t. Differentiation of eq. (5), followed by rearranging, yields an expression for the desorption rate R_{des}:

$$R_{des} = -\frac{\varepsilon_s \rho_{hydr}}{2M_{hydr}} \frac{dF}{dt} = \frac{\varepsilon_s \rho_{hydr}}{2M_{hydr}} 3k_d \ln\left(\frac{C_{eq,d}}{C_{H_2,s}}\right) F_0^{1/3} F^{2/3}. \quad (16)$$

The desorption rate is equal to $R_{C_6H_{10}} - J_{H_2}a$ [eq. (1)], whereas $J_{H_2}a$ is in this case related to the pressure drop in the reactor according to

$$J_{H_2}a = -\frac{V_{r,g}}{z_r R T_r V_{sl}} \frac{dP_{H_2}}{dt}. \quad (17)$$

Since $R_{C_6H_{10}}$, $J_{H_2}a$ and F [eq. (12), shown in Fig. 8(b)] can be obtained from experimental data, the surface concentration $C_{H_2,s}$ is the only unknown parameter. Further rearranging of eq. (16) provides a relation for $C_{H_2,s}$:

$$C_{H_2,s} = C_{eq,d} / \exp\left[\frac{2M_{hydr}(R_{C_6H_{10}} - J_{H_2}a)}{\varepsilon_s \rho_{hydr} 3k_d F_0^{1/3} F^{2/3}}\right]. \quad (18)$$

With the experimental datapoints as depicted in Figs 8(a) and (b) and eqs (17) and (18), the surface concentration has been obtained, as shown in Fig. 12. The largest difference between $C_{H_2,s}$ and $C_{eq,d}$ is found at the start of an experiment. Here the hydrogenation rate is somewhat limited by the transport of hydrogen from the centre of the hydride particles to the surface. At increasing cyclohexene conversion, the difference becomes relatively small and almost constant. The hydrogenation rate is now almost completely limited by the reaction between the adsorbed cyclohexene and hydrogen.

The values for $C_{H_2,s}$ and the cyclohexene concentrations can also be substituted in eq. (15). For the hydrogenation on the α and on the β phase of $LaNi_5$, the fitted values ($k_r a_s$ and $K_{C_6H_{10}}$) as listed in Table 3 have been used. The derived theoretical reaction rates can be compared with the experimentally observed rates as demonstrated in Fig. 13. It is clear that the experimental reaction rate varies between the two theoretical rates. Since the $LaNi_5$ is initially (high cyclohexene concentration) completely in β phase, it is to be expected that the experimental rate is in good agreement with the theoretical rate for the hydrogenation on the β phase of the $LaNi_5$. Since the liquid is saturated at the absorption equilibrium pressure, the initial hydrogen concentration in the solvent is higher than that calculated according to eq. (18). This explains the somewhat higher experimental rate at the start of the experiment. During the reaction hydrogen is consumed and the hydride particles are gradually

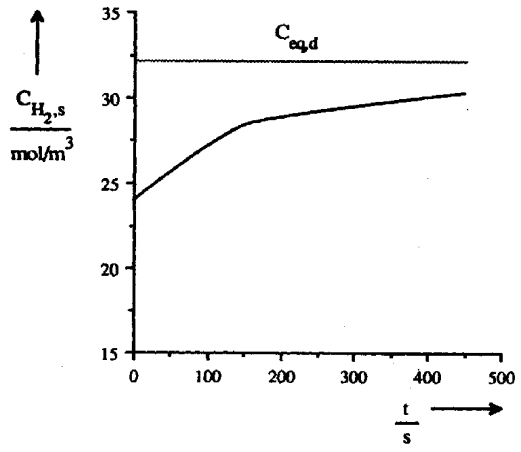

Fig. 12. Calculated hydrogen concentration close to the surface according to eq. (18).

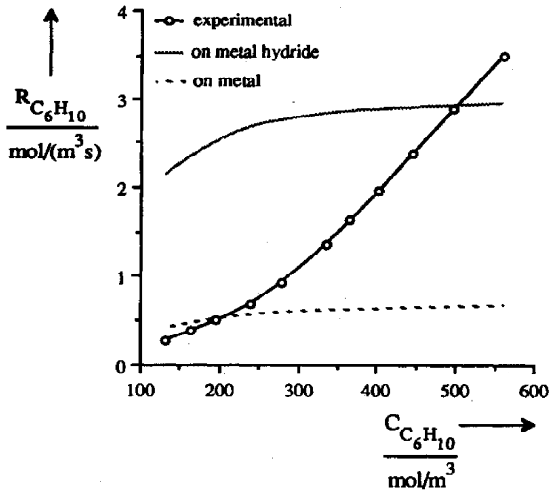

Fig. 13. Comparison between the measured and the calculated hydrogenation rates when hydrogen is provided by $LaNi_5H_n$.

converted into the α phase of $LaNi_5$. The reaction proceeds on these particles according to the lower curve in Fig. 13. The change in the nature of the particle surface from the β to the α phase during the hydrogenation of cyclohexene is apparently the reason for the continuous decrease of the reaction rate.

5. CONCLUSIONS

The mechanism and kinetics of cyclohexene hydrogenation on $LaNi_{5-x}Al_xH_n$, with $x = 0$, 0.1 and 0.2, have been investigated in a slurry reactor. Hydrogenation experiments were carried out with hydrogen supplied by the gas phase or by the metal hydride. The mechanism could be described with a Langmuir–Hinshelwood type of kinetic equation, assuming a fast dissociative adsorption of hydrogen and adsorption of cyclohexene on two different sites:

$$R_{C_6H_{10}} = k_r a_s \sqrt{C_{H_2,s}} \frac{K_{C_6H_{10}} C_{C_6H_{10}}}{1 + K_{C_6H_{10}} C_{C_6H_{10}}}.$$

Both the reaction rate constant and the adsorption coefficient for cyclohexene decrease at increasing aluminum content in the alloy. Also, a reduction of the reaction rate and adsorption coefficient was found when the material changes from the β phase into the α-phase. Using ethanol as solvent results in a higher reaction rate constant than in cyclohexane, but the adsorption coefficient is lower.

The hydrogenation of cyclohexene with hydrogen provided by the $LaNi_5$ hydride can be described according to a mechanism which combines the rate equation for the hydrogenation and the relation for desorption of hydrogen form the metal hydride particles. As the reaction proceeds, the surface of the particles changes from the β into the α phase; consequently, the reaction rate decreases continuously. Initially, the hydrogenation rate is partly limited by the transport of hydrogen from the bulk of the particles to the surface, but at higher cyclohexene conversions the rate is limited by the surface reaction.

Acknowledgements—These investigations were supported by the Foundation for Chemical Research in the Netherlands (S.O.N.) and DSM. We also acknowledge H. J. Bakker, J. W. Dijkstra, Y. J. R. van Es, W. de Jong and T. D. Nauta for their contribution to the experimental work, and K. van Bree, S. Kuipers, A. H. Pleiter, A. Schanssema and H. J. Vunderink for their technical support.

NOTATION

a	specific interfacial area, m^2/m^3_{slurry}
A_{hydr}	surface area of the metal particles, m^2/kg
C	concentration, mol/m^3
d_p	particle diameter, m
F	hydrogen absorption capacity, number of H atoms/La atom
ΔH_a	heat of adsorption, kJ/mol
J	molar flux, $mol/(m^2\,s)$
k_d	reaction rate constant for desorption, 1/s
k_r	reaction rate constant based on surface area, $mol^{0.5}/(m^{0.5}\,s)$
k_4	reaction rate constant based on surface area, $mol/(m^2\,s)$
k_l	gas–liquid mass transfer coefficient (hydrogen), m/s
k_s	liquid–solid mass transfer coefficient (hydrogen), m/s
k'_s	liquid–solid mass transfer coefficient (cyclohexene), m/s
K	adsorption coefficient, m^3/mol or $m^{1.5}/mol^{0.5}$
m	solubility coefficient $(=C_{H_2,l}/C_{H_2,g})_{eq}$, dimensionless
M	molecular mass, kg/mol
n	number of moles, mol
n	stirrer speed, rpm
P	pressure, bar
R	reaction rate, $mol/(m^3_{slurry}\,s)$
R	gas constant, 8.3143 J/(mol K)
t	time, s
T	temperature, K
V	volume, m^3
X	fraction reacted, dimensionless
z	compressibility factor, dimensionless

Greek letters

ε	volume fraction, dimensionless
ρ	density, kg/m^3
χ	minimization function, $mol/(m^3\,s)$

Subscripts/superscripts

a	absorption
d, des	desorption
eq	equilibrium
g	gas
hydr	hydride
i	at the interface
l	liquid
r	reactor
s	solid

sl	slurry
vap	vapour
0	at $t = 0$

REFERENCES

Appelman, W. J. T. M., Kuczinsky, M. and Versteeg, G. F., 1992, Simultaneous dehydrogenation of organic compounds and hydrogen removal by hydride forming alloys. *Appl. Catal.* **81**, 35–46.

Baglin, E. G., Atkinson, G. B. and Nicks, L. J., 1981, Methanol synthesis catalysts from thorium–copper intermetallics. Preparation and evaluation. *Ind. Engng Chem. Prod. Res. Dev.* **20**, 87–90.

Barbernics, L. and Tétényi, P., 1972, Investigation of the adsorption of benzene and cyclohexane on metallic Ni and NiO. *Z. Phys. Chem. N.F.* **82**, 262–271.

Barrault, J., Guilleminot, A., Achard, J. C., Paul-Boncour, V., Percheron-Guegan, A., Hilaire, L. and Coulon, M., 1986, Syngas reaction over lanthanum–cobalt intermetallic catalysts. *Appl. Catal.* **22**, 273–287.

Bond, G. C., 1962, *Catalysis by Metals.* Academic Press, London.

Chesters, M. A., Parker, S. F. and Raval, R., 1986, Cyclohexane adsorption on Cu(111) studied by infrared and electron energy loss spectroscopy. *J. Electron Spectrosc. Relat. Phenom.* **39**, 155–162.

Coon, V. T., Takeshita, T., Wallace, W. E. and Craig, R. S., 1976, Rare earth intermetallics as catalysts for the production of hydrocarbons from carbon monoxide and hydrogen. *J. phys. Chem.* **80**, 1878–1879.

Gonzo, E. E. and Boudart, M., 1978, Catalytic hydrogenation of cyclohexene III. Gas phase and liquid phase reaction on supported palladium. *J. Catal.* **52**, 462–471.

Goodell, P. D., 1984, Stability of rechargeable hydriding alloys during extended cycling. *J. Less-Common Met.* **99**, 1–14.

Holstvoogd, R. D., van Swaaij, W. P. M., Versteeg, G. F. and Snijder, E. D., 1989, Continuous absorption of hydrogen in metal hydride slurries, *Z. Phys. Chem. N.F.* **164**, 1429–1434.

Imamura, H., Yamada, K., Nukui, K. and Tsuchiya, S., 1986, Dehydrogenation reactions of organic compounds using hydrogen-absorbing rare earth intermetallic compounds. *J. Chem. Soc. chem. Commun.*, 367–368.

Imamoto, T., Mita, T. and Yokoyama, M., 1987, Reduction of organic compounds with rare-earth intermetallics containing absorbed hydrogen. *J. org. Chem.* **52**, 5695–5699.

Imamura, H., Takada, T., Kasahara, S. and Tsuchiya, S., 1990, Efficient dehydrogenation of methanol using hydride-forming alloys (Zr_2Ni, R_2Co_7 and RFe_2) as hydrogen acceptors. *Appl. Catal.* **58**, 165–173.

Madon, R. J., O'Connel, J. P. and Boudart, M., 1978, Catalytic hydrogenation of cyclohexene II. Liquid phase reaction on supported platinum in a gradient less slurry reactor. *A.I.Ch.E. J.* **24**, 904–911.

Mal, H. H. van and Miedema, A. R., 1978, Some applications of $LaNi_5$-type hydrides, in *Hydrogen for Energy Storage* (Edited by A. F. Andressen and A. J. Maeland), pp. 251–260. Pergamon Press, Oxford.

Martin, G. A. and Imelik, B., 1974, Adsorption of hydrocarbons and various gases on Ni–SiO_2 catalysts studied by high field magnetic methods. *Surf. Sci.* **42**, 157–172.

Press, W. H., Flannery, B. P., Teukolsky, S. A. and Vetterling, W. T., 1986, *Numerical Recipes, the Art of Scientific Computing.* Cambridge University Press, Cambridge.

Reilly, J. J., 1977, Metal hydrides as hydrogen storage media and their applications, in *Hydrogen, Its Technology and Implications* (Edited by K. E. Cox and K. D. Williamson), Vol. 2, pp. 13–48. CRC Press, Cleveland.

Segal, E., Madon, R. J. and Boudart, M., 1978, Catalytic hydrogenation of cyclohexene I. Vapour phase reaction on supported platinum. *J. Catal.* **52**, 45–49.

Shamsi, A. and Wallace, W. E., 1983, Synthesis gas reaction over oxidized intermetallic compounds. *Ind. Engng Chem. Prod. Res. Dev.* **22**, 582–587.

Snijder, E. D., Versteeg, G. F. and van Swaaij, W. P. M., 1992, The kinetics of hydrogen absorption and desorption in $LaNi_{5-x}Al_x$ slurries. *A.I.Ch.E. J.* (accepted).

Soga, K., Imamura, H. and Ikeda, S., 1979, Hydrogenation of ethylene over some intermetallic compounds. *J. Catal.* **56**, 119–126.

Svoboda, J., Rocková, E. and Kochloefl, K., 1970, Gas chromatographic study of hydrocarbon adsorption on nickel catalysts. *Colln Czech. Chem. Commun.* **35**, 1671–1686.

Takeshita, T., Wallace, W. E. and Craig, R. S., 1976, Rare earth intermetallics as synthetic ammonia catalysts. *J. Catal.* **44**, 236–243.

Wallace, W. E., Karlicek, R. F. and Imamura, H., 1979, Mechanism of hydrogen absorption by $LaNi_5$. *J. phys. Chem.* **83**, 1708–1712.